PHYSICAL REVIEW B VOLUME 45, NUMBER 8 15 FEBRUARY 1992-II

# Ternary nitrides $BiNCa_3$ and $PbNCa_3$: Unusual ionic bonding in the antiperovskite structure

D. A. Papaconstantopoulos and W. E. Pickett
*Complex Systems Theory Branch, Naval Research Laboratory, Washington, D.C. 20375-5000*

(Received 17 June 1991)

The compounds $BiNCa_3$ and $PbNCa_3$, a narrow-gap semiconductor and a metal, respectively, with the antiperovskite structure, are investigated with the local-density augmented-plane-wave method. The calculations confirm that both N and the heavy ions Bi and Pb are close to the nominal 3− charge states of an ionic picture; however, there is considerable covalent mixing between the two sets of *p* states. The filled *p* bands of the $BiNCa_3$ compound are separated from the conductions bands, with a calculated gap of ~0.1 eV consistent with its semiconducting behavior. $PbNCa_3$, with one less electron per cell and therefore an unfilled *p* band, is predicted correctly to be metallic, consistent with a rigid-band picture.

## I. INTRODUCTION

Oxygen-based perovskites display a wide range of physical properties, from wide-gap insulators to ferroelectrics and superconductors, as well as a wide range of structural instabilities. Recently, DiSalvo and collaborators[1,2] have synthesized a class of antiperovskites, $XNCa_3$, based on nitrogen and using calcium as a cation, which assumes the role of the oxygen atom in perovskites. The perovskite-antiperovskite distinctions are striking: $O^{2-}$, with its ionic radius of 1.2 Å and highly polarizable *p* shell, forms the ionic "glue" for a wide variety of perovskites with cations of varying sizes. In the antiperovskite its site is occupied by the $Ca^{2+}$ ion, its small ionic radius of 1.0 Å allowing it to accommodate large anions in this structure. The antiperovskite crystal structure, with atom sizes approximately reflecting the ionic sizes, is shown in Fig. 1.

Antiperovskite ternary nitride compounds have been synthesized by DiSalvo and co-workers with the element $X$ taken from either group V ($X$=Bi,Sb,As,P) or group IV ($X$=Pb,Sn,Ge). Based both on the stoichiometry and the interatomic distances, these compounds appear to follow the formal ionic picture $X^{3-}N^{3-}(Ca^{2+})_3$, in which case the group-V elements (including N) will be closed-shell ions and the compound would be nonmetallic, as observed. The group-IV elements will present unfilled *p* shells (and an odd number of electrons per unit cell), consistent with their observed metallic behavior.

We review briefly what is known[1,2] about this class of materials. The Pb, Sn, and Ge compounds are cubic and metallic. The Bi, Sb, As, and P compounds are nonmetals, with the first two classed as semiconductors and the last two as insulators. The behavior of the nonmetals is consistent both with their color (black, gray, red, and yellow, respectively) and their increasing electronegativity (Bi→Sb→As→P), which would suggest an increasing band gap. Not only are the As and P compounds insulators, they are observed to have a small orthorhombic distortion away from the cubic perovskite structure, thought to result from their smaller ionic radii (they are too small to fill the available hole completely). Due to the difficulty in making these compounds and their sensitivity to air, this information is all that is currently available.

The 3− charge states of Bi and Pb are highly unusual, especially in a nitride. These atoms are sometimes formally anionic, as in $Na_3Bi$, $Ca_3Bi_2$, or CaPb, but highly anionic oxidation states have not been observed in compounds with highly electronegative elements. Nitrogen itself is highly electronegative, midway between S and O and similar to Cl, and the other group-V elements are considerably less so. Yet these group-IV and -V elements appear to behave as highly electronegative ions in these antiperovskite compounds.

The discovery of these compounds has prompted us to initiate a study of their electronic structure and bonding properties. We have chosen to begin with the pair of compounds $BiNCa_3$ and $PbNCa_3$, for several reasons.

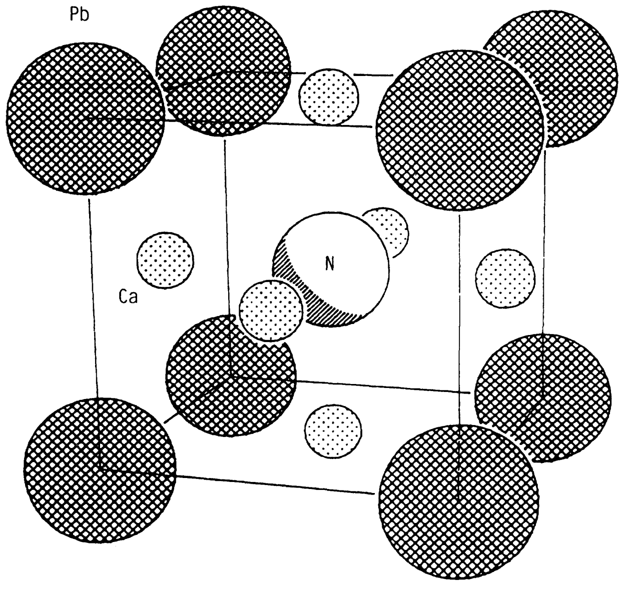

FIG. 1. The antiperovskite crystal structure.

First of all, they are cubic, and this simplifies not only the calculation but the interpretation as well. Second, Bi and Pb are neighbors in the Periodic Table, so the electronic structures of the respective compounds will be very similar in most respects. Thirdly, there is somewhat more experimental information on these two compounds (e.g., temperature dependence of resistivity of the Bi material) than on similar pairs. Fourth, there has been increasing interest, both in our group and elsewhere, on the electronic structure of ionic Bi compounds, especially in the perovskite structure, and the study of this compound will provide information about the behavior of Bi in such solids.

The calculational method is described in the following section, with the analysis of the electronic structure given in Sec. III. A brief discussion and mention of remaining questions are presented in Sec. IV.

## II. METHOD OF CALCULATION

These calculations were performed by the augmented-plane-wave (APW) method[3] in the muffin-tin (MT) approximation with the lattice constants and MT sphere radii given in Table I. These radii were determined by the following expressions: $R_N = R_{Ca} = a/4$ and $R_{Bi(Pb)} = a\sqrt{2}/2 - a/4$, which result in 53% of the total unit-cell volume enclosed within the MT spheres. The MT approximation introduces only a small error for cubic systems, unlike the more open structures, where a full potential treatment is necessary. The APW calculations were performed in a scalar-relativistic approximation i.e., they treat exactly the mass-velocity and Darwin terms of the Hamiltonian, but neglect the spin-orbit interaction term. In Table II the states that were calculated as bands in the APW calculation are shown. The inner levels were recalculated in each iteration (soft-core calculation) by a relativistic atomic-structure program that handles exactly the spin-orbit interaction. The prescription of Hedin and Lundqvist[4] was used to treat exchange and correlation in the local-density approximation for both inner and outer energy levels. A uniform mesh of 10 **k** points in $\frac{1}{48}$ of the Brillouin zone (BZ) was used through 20 cycles until self-consistency was achieved. The final iteration was performed for 35 **k** points to provide an adequate sampling for the interpolation. The interpolation of the eigenvalues $E(k)$ and of the electronic charges inside the MT spheres, $Q_l(k,E)$, was done using the Fourier-series scheme of Boyer,[5] which takes into account the symmetry of the bands, handling band crossings correctly. The interpolated $E(k)$ and $Q_l(k,E)$ are given on a mesh of 969 **k** points, which, in turn, are used as an input to calculate the densities of states by the tetrahedron method.[6]

TABLE I. Lattice constants $a$ and muffin-tin radii $R$ (in atomic units) that were used in the augmented-plane-wave calculations.

| | $BiNCa_3$ | $PbNCa_3$ |
|---|---|---|
| $a$ | 9.240 76 | 9.278 56 |
| $R_{Bi(Pb)}$ | 4.224 01 | 4.241 29 |
| $R_N$ | 2.310 19 | 2.319 64 |
| $R_{Ca}$ | 2.310 19 | 2.319 64 |

TABLE II. Semicore and valence levels calculated as bands by the APW method.

| | | | |
|---|---|---|---|
| Pb | 5*d* | 6*s* | 6*p* |
| Bi | | 6*s* | 6*p* |
| N | 2*s* | 2*p* | |
| Ca | 4*s* | | |

## III. ANALYSIS OF ELECTRONIC STRUCTURE

In Figs. 2(a) and 2(b) we show the band structures of $BiNCa_3$ and $PbNCa_3$, respectively, and the site-decomposed local densities of states (LDOS's) and total DOS's are shown in Figs. 3(a) and 3(b). The N 2*s* semicore band is centered ~12.5–13 eV below the Fermi level ($E_F$) in each compound and is nearly 1 eV wide. The 6*s* states of Bi and Pb lie 10.5 and 8 eV below $E_F$, respectively, and have widths somewhat less than 1 eV. These corelike states are not expected to participate appreciably in the bonding of the crystals.

The striking difference in the materials is that $BiNCa_3$ is predicted to be a narrow-gap semiconductor, with $E_g = 0.07$ eV, while $PbNCa_3$ is a moderately high-DOS metal, with $N(E_F) = 3.16$ states/eV cell. This is qualitatively in agreement with the experimental findings.[2] For a qualitative picture a rigid-band model based on the $BiNCa_3$ band structure is sufficient; for the Bi compound the number of valence electrons is just sufficient to fill all states below the gap, while the Pb compound, having one fewer electron per cell, has its Fermi level falling about 1 eV lower in a region of overlapping bands. The differences between the band structures (non-rigid-band effects) will be discussed below.

### A. $BiNCa_3$

The first question to address is whether the band gap of $BiNCa_3$ is primarily ionic or covalent in character. On one hand, $Bi^{3-}N^{3-}(Ca^{2+})_3$ satisfies the formal valence requirements of an ionic insulator. On the other hand, purely ionic insulators are usually *wide-gap* insulators. A look at the LDOS curves answers this question. The amount of Ca contribution to the occupied states is quite small and likely best interpreted as reflecting the tails of states on neighboring atoms protruding into the Ca sphere. Consequently, Ca is close to its normal $Ca^{2+}$ ionic configuration.

The six occupied valence bands of width 4 eV are comprised of N 2*p* and Bi 6*p* states, each contributing about equally to the total number of valence electrons. If this is true, then each is a triply negative ion, implying that the ionic picture with full formal ionicity $[Bi^{-3}N^{-3}(Ca^{+2})_3]$ is appropriate. This ionic picture is not an accurate one without further modification, however, as we now discuss.

The DOS curves reveal a three-peak structure in the valence-band DOS, with peaks near −4 eV, −2 eV (very sharp), and −1 eV, relative to the valence-band maximum at Γ (hereafter taken as the zero of energy). Bi 6*p* states contribute to all three peaks, but most strongly to only the two most weakly bound peaks, while N 2*p* states contribute only to the peaks at −4 and −2 eV. Thus, the states in the upper 1 eV of the occupied bands are dominantly Bi 6*p* character, while the other peaks contain both Bi and N character. The middle peak arises from a band that is extremely flat along all symmetry directions (except a small region of anticrossing along the Λ direction). From the LDOS it is clear that this band has strongly hybridized Bi 6*p*−N 2*p* character, as do all of the four lower valence bands (over nearly all of Brillouin zone). Therefore, there is strong *covalent mixing* occurring between the Bi and N *p* states.

Although the Bi and N *p* bands are well hybridized, the gap is not a covalent, bonding-antibonding gap because all of the combined *p* bands (both bonding and antibonding) are occupied. The most strongly bonding combination lies at the zone-edge, *M*, and corner, *R*, points, while the antibonding combination occurs at Γ and forms the lower gap edge. The N and Bi sublattices of the perovskite structure form a CsCl substructure. When the Ca sublattice is considered, the N and Bi sites become inequivalent in symmetry and chemistry, with the N site

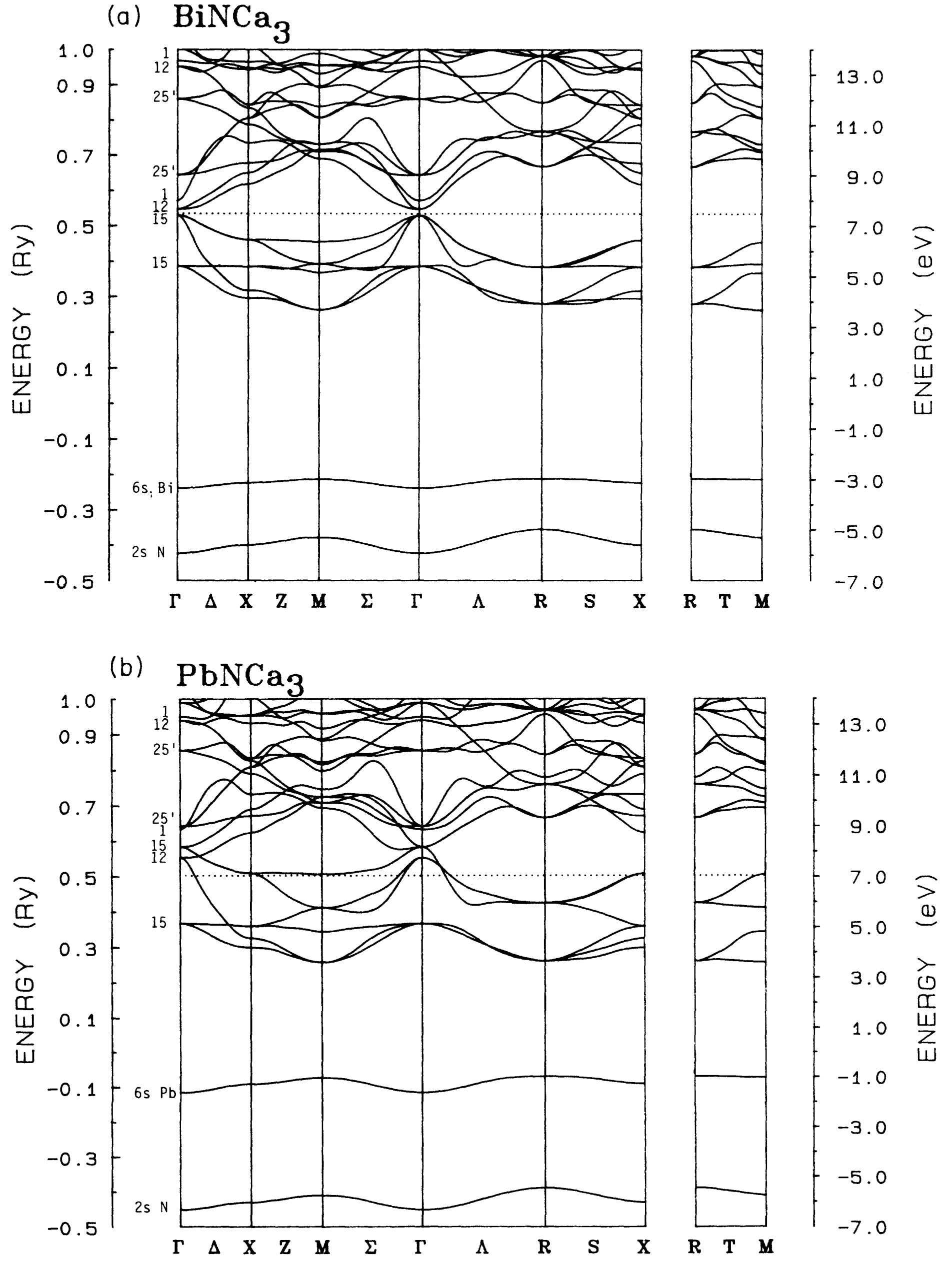

FIG. 2. Band structure of (a) $BiNCa_3$ and (b) $PbNCa_3$, along the principal high-symmetry directions in the Brillouin zone. The dotted line denotes the valence-band maximum and Fermi level, respectively.

being sixfold coordinated to Ca ions at distance $a/2$, while the Bi site is twelvefold coordinated to Ca at distances of $\sqrt{2}a/2$. The Madelung potential of the $\mathrm{Ca}^{2+}$ sublattice is less attractive for electrons at the N site than the Bi site, but the greater electronegativity of N accounts for the predominance of N $p$ character in the lower valence bands.

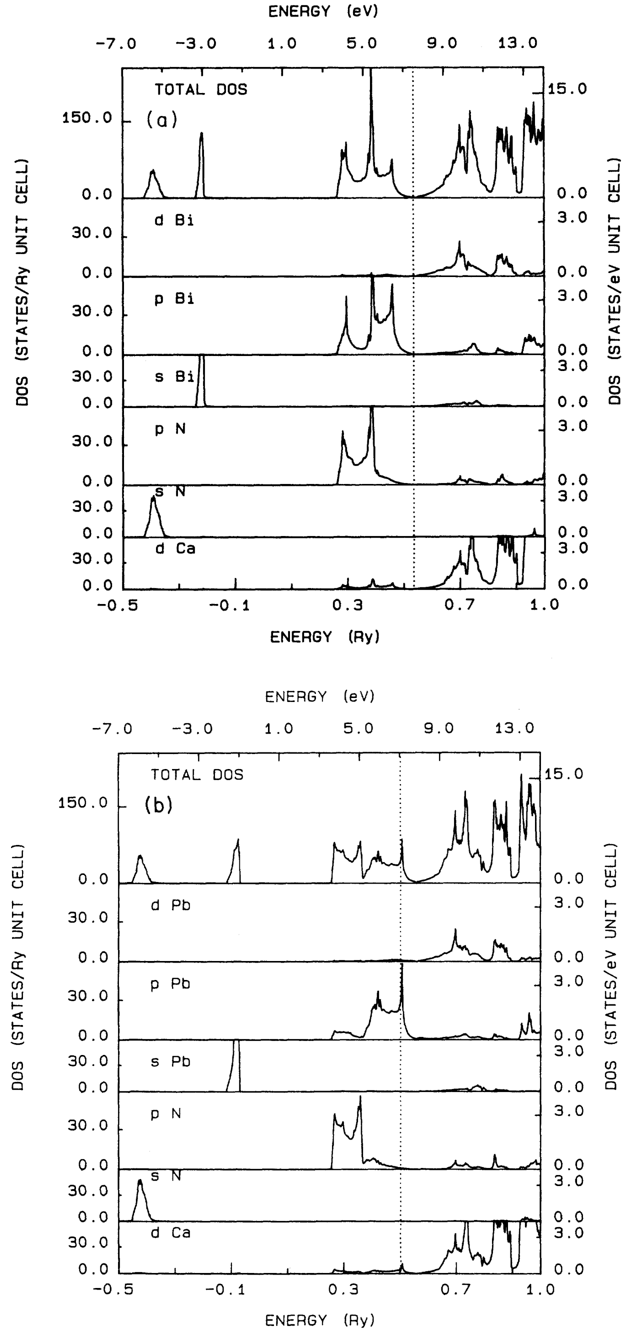

FIG. 3. Total and angular-momentum-decomposed atomic densities of states for (a) $\mathrm{BiNCa_3}$ and (b) $\mathrm{PbNCa_3}$. Local densities of states that are not shown are much smaller than those that are presented. Note that these densities of states reflect the volume within the sphere (given in Table I), so comparison of values should be done with caution.

The conduction bands are of entirely different character. From the wave functions we learn that the lowest conduction band, $\Gamma_{12}$, contains about 70% Bi $d$-$e_g$ and 30% Ca $3d$-$e_g$ character in a bonding combination. The next higher $\Gamma_{12}$ state is nearly 6 eV above $E_F$ and is entirely Ca $d$-$e_g$. Around 2 eV above the valence-band maximum, the $d$-$t_{2g}$ character of Bi and Ca rises sharply, but the Ca $d$-$t_{2g}$ fraction rapidly becomes dominant.

Two $\Gamma_{25'}$ states occur at about 2 and 5 eV above $E_F$, with 75/25 and 80/20 ratios of Ca/Bi $d$-$e_g$ character, respectively. Since there are (unoccupied) $d$ states on the Bi and each of three Ca ions, there will be ten more $d$ states at higher energy than the bands we have included in Fig. 2. The symmetric state, $\Gamma_1$, at $\sim 1$ eV, is an 80/20 ratio of Bi/Ca $s$ character.

The fundamental gap occurs, therefore, between an antibonding combination of Bi and N $\Gamma_{15}$ $p$ states and a bonding combination of Bi and Ca $d$-$e_g$ states. Since both states contain a majority of Bi character and the Bi $p \rightarrow$Bi $d$ transition is optically allowed, a clear identification of the gap by optical means should be possible. Although the compound is ionic, the gap is small because (i) Bi is a large-$Z$ atom in which the $6d$ states are near the $6p$ states, and (ii) because the $\mathrm{Ca}^{2+}$ ion has $d$ states at rather low energy. Note, however, that over much of the BZ the gap is of the order of 4 eV.

### B. $\mathrm{PbNCa_3}$

Since Pb has one fewer electron than Bi and since $\mathrm{BiNCa_3}$ is insulating, one expects $\mathrm{PbNCa_3}$ to be metallic with the Fermi level $E_F$ lying below the gap. From Fig. 2(b) that is indeed seen to be the case, except that the gap has closed due to a rearrangement of the self-consistent potential in response to the "replacement" of Bi by Pb. The remnant of the gap is seen in the nearly vanishing DOS (pseudogap) about 0.8 eV above $E_F$.

Generally, the orbital characters of states at $\Gamma$ in $\mathrm{PbNCa_3}$ are very similar to those in $\mathrm{BiNCa_3}$. The gap in $\mathrm{BiNCa_3}$ has closed in $\mathrm{PbNCa_3}$ due to the interchange in energies of the upper $\Gamma_{15}$ state and the lower $\Gamma_{12}$ state. This reversal is likely a result of the greater lowering of the $6p$ state in Bi compared to Pb, than occurs for the $6d$ state.

Several other differences are evident. The valence-band width (up to the pseudogap) has increased to nearly 5 eV, and the pronounced three-peak structure in $\mathrm{BiNCa_3}$ has disappeared. Instead, the valence DOS is nearly split into two parts, with the lower 2 eV being predominantly N $2p$ and the upper 3 eV being predominantly Pb $6p$. The Fermi level falls very near a sharp peak in the DOS arising from a very flat band along the zone edge $X$-$M$. As for $\mathrm{BiNCa_3}$, the occupied Ca character is very small, while the N $2p$ bands are entirely filled. This suggests the formal description $\mathrm{Pb}^{3-}\mathrm{N}^{3-}(\mathrm{Ca}^{2+})_3$, which is consistent with metallic behavior since $\mathrm{Pb}^{3-}$ is not a closed-shell ion. In Table III the decomposition of DOS at $E_F$ is given. The main contributions at $E_F$ are Pb$p$-like and Ca $t_{2g}$.

TABLE III. Values of the densities of states at the Fermi level for $PbNCa_3$, decomposed by site and symmetry. Note that the $l$-components correspond to the volume inside the muffin-tin spheres. Units are states/Ry cell both spins.

| | $s$ | $p$ | $e_g$ | $t_{2g}$ |
|---|---|---|---|---|
| Pb | 0.11 | 27.32 | 0.92 | 0.09 |
| N | 0.01 | 0.86 | 0.00 | 0.14 |
| Ca | 0.11 | 0.72 | 0.73 | 4.37 |
| Total | 42.94 | | | |

The conduction bands of $PbNCa_3$ (those above the pseudogap) strongly resemble those of $BiNCa_3$; for example, the bands along the zone edge $R$-$M$ are nearly identical. The most noticeable difference is the change in ordering of levels at $\Gamma$ of the second and third eigenvalues, which, in fact, is responsible for the closing of the gap. The relative shift of these two bands (between the Bi- and Pb-based compounds) is less than 1 eV, and the accompanying shift or overlap of Pb $p$ with Ca $d$ character is not visible in the LDOS plots due to the small phase space.

Our analysis indicates that $PbNCa_3$ is a strongly ionic metal, not unlike the high-temperature Cu-O superconductors, except that the Fermi-level DOS $N(E_F)$ is substantially larger. The metallic electrons are confined primarily to the Pb sublattice, which is intertwined with the positively and negatively charged $Ca^{2+}$ and $N^{3-}$ sublattices. In analogy with the Cu-O superconductors, $PbNCa_3$ can be expected to display electron-phonon interaction with important contributions from nonlocal (Madelung) effects, which will lead to coupling to N-ion displacements in spite of the very low Fermi-level DOS on this ion. The coupling of the Pb, and to a lesser extent the Ca, ions may be more strongly screened, in which case a rigid-muffin-tin model can be used as a first estimate of their electron-phonon coupling strength. The rigid-muffin-tin values of $\eta_a = N(E_F)\langle I_a^2\rangle$ are 0.15, 0.07, and 0.35 eV/Å$^2$ for the Pb, N, and three Ca atoms, respectively.

These values may be compared with those of a superconducting perovskite, $BaPb_{0.6}Bi_{0.4}O_3$, that has been studied previously.[7,8] Although $N(E_F)$ is more than a factor of 3 smaller, the values of $\eta_a = 0.0$, 0.5, and 1.3 eV/Å$^2$ for Ba, Pb-Bi, and $O_3$, respectively, are much stronger overall. Therefore the electron-ion scattering matrix elements $\langle I_a^2\rangle$ are *much* weaker in $PbNCa_3$, accounting for the lack of superconductivity in this nitride compound.

## IV. DISCUSSION

The occurrence of a sharp, high-DOS peak at $E_F$ suggests a tendency toward a lattice distortion that would split the peak and stabilize the electronic system by lowering $N(E_F)$. Since $N(E_F)$ is primarily derived from Pb states in an antibonding relation to the N $p$ states, a breathing-type distortion (common in perovskites) that makes the N ions inequivalent might result in a splitting of the peak at $E_F$. Experimentally no such distortion has been seen.

A potentially important effect we have not considered here is spin-orbit (SO) coupling. For $p$ states in crystalline Pb, SO coupling causes band shifts of the $\Gamma_{15}$ states of the order of 1 eV. Including SO coupling would be expected to split the $\Gamma_{15}$ states by a comparable amount, reduced according to the fraction of Pb $p$ character in the state (SO coupling in N is negligible). Thus, including SO coupling should alter the peak structure in $N(E)$ near the $\Gamma_{15}$ states (and to a lesser extent for the $\Gamma_{12}$ and $\Gamma_{25'}$ states).

A more important effect of SO coupling may occur in $BiNCa_3$, where splitting of the $\Gamma_{15}$ and $\Gamma_{12}$ states bordering the gap could result in band overlap at $\Gamma$. Even if this were to occur, it is possible that hybridization in the band-(anti)crossing regions away from $\Gamma$ could yet result in a small semiconducting gap. Although band methods are available to deal with SO coupling starting with the semirelativistic approximation[9] that we have applied, this method is still only approximate for $6p$ states. An accurate exposition of the band structure of $BiNCa_3$ in the gap region may require a fully relativistic (Dirac) calculation.

## ACKNOWLEDGMENTS

We are indebted to F. J. DiSalvo for extensive discussions of these materials as well as for providing Fig. 1. This work was supported by the Office of Naval Research.

---

[1] F. J. DiSalvo, Science **247**, 649 (1990).

[2] M. Y. Chern, D. A. Vennos, and F. J. DiSalvo, J. Solid State Chem. (to be published).

[3] L. F. Mattheiss, J. H. Wood, and A. C. Switendick, Methods Comput. Phys. **8**, 63 (1968).

[4] L. Hedin and B. I. Lundqvist, J. Phys. C **4**, 2064 (1971).

[5] L. L. Boyer, Phys. Rev. B **19**, 2824 (1979).

[6] G. Lehmann and M. Taut, Phys. Status Solidi B **54**, 469 (1972).

[7] D. A. Papaconstantopoulos, A. Pasturel, J. P. Julien, and F. Cyrot-Lackmann, Phys. Rev. B **40**, 8844 (1989).

[8] J. P. Julien, D. A. Papaconstantopoulos, F. Cyrot-Lackmann, and A. Pasturel, Phys. Rev. B **43**, 2903 (1991).

[9] A. H. MacDonald, W. E. Pickett, and D. D. Koelling, J. Phys. C **13**, 2675 (1980).